Hindawi
Journal of Chemistry
Volume 2019, Article ID 2949316, 8 pages
https://doi.org/10.1155/2019/2949316

Research Article

Enhanced Photocatalytic Degradation of Rhodamine B Using C/Fe Co-Doped Titanium Dioxide Coated on Activated Carbon

Thuy Le Thi Thanh,[1] **Lan Nguyen Thi**,[1] **Trinh Tran Dinh**,[2,3] **and Noi Nguyen Van**[2,3]

[1]*Department of Chemistry, Faculty of Science, Qui Nhon University, No. 170 An Duong Vuong Street, Qui Nhon, Vietnam*
[2]*Faculty of Chemistry, VNU-University of Science, No. 19 Le Thanh Tong Street, Hanoi, Vietnam*
[3]*VNU Key Laboratory of Advanced Materials for Green Growth, No. 334 Nguyen Trai Street, Hanoi, Vietnam*

Correspondence should be addressed to Thuy Le Thi Thanh; lethithanhthuy@qnu.edu.vn and Trinh Tran Dinh; trinhtd@vnu.edu.vn

Received 15 March 2019; Accepted 21 May 2019; Published 23 June 2019

Academic Editor: Mallikarjuna N. Nadagouda

Carbon and iron co-doped titanium dioxide catalyst coated on activated carbon (Fe-C-TiO_2/AC) was successfully synthesized using the sol-gel method, followed by hydrothermal treatment. Commercial activated carbon was treated by HNO_3 prior to being coated by the as-synthesized catalyst. The composite was characterized by XPS, XRD, UV-Vis spectrophotometry, IR, TEM, HR-TEM, and BET. The performance of the supported catalysts was evaluated in the degradation of rhodamine B (RhB) in the solution under visible-light irradiation. The results showed that, with the appropriate amount of activated carbon, prepared Fe-C-TiO_2/AC catalysts exhibited higher catalytic activities and Fe-C-TiO_2/AC system showed the best performance. The photocatalytic degradation efficiency of Fe-C-TiO_2/AC was enhanced due to the synergistic effect between AC (adsorption effect) and Fe-C-TiO_2 (photocatalysis effect). This facilitated the photocatalytic degradation of RhB by Fe-C-TiO_2.

1. Introduction

TiO_2 photocatalyst has been widely used in the wastewater treatment and other environmental remediation because of its high efficiency, nontoxicity, propitious recycle ability, and low cost. Besides, the final products of the photocatalysis in the advanced oxidation process are CO_2, H_2O, inorganic ions, and minerals that usually have insignificant impacts on environments [1, 2]. However, the application of TiO_2 is limited because the TiO_2 with band gap ~3.2 eV is only activated under UV radiation and it is difficult to recycle. Therefore, modification of catalyst is crucial to enhance its photocatalytic activity. To present, catalytic efficiency of TiO_2 was significantly improved by being doped with metals such as V, Cr, W, and Fe or with metal oxides like ZnO, CuO, and so on for expanding the absorption edge to the visible region [3–6]. Among these metals, TiO_2 doped with Fe is in progress because Fe can replace the positions of Ti^{4+} in the crystalline, reducing the band gap energy, which is conducive to the activation in the visible light [3, 4, 7]. Moreover, Fe ions act as traps to incarcerate electrons and hinder the recombination of electron/hole pairs, resulting in the increase in catalysts' performance. In addition, the addition of some nonmetal elements such as N, C, S, P, and halogens into TiO_2 structure can also narrow the band gap of TiO_2, reinforcing the photocatalytic activity of the catalyst [2, 8]. Some research reported that transition metals/(N, C, S) co-doped into TiO_2 would greatly facilitate the photocatalytic performance of the corresponding catalysts under visible irradiation conditions, which was attributed to the synergistic effects between the doped C and N atoms and lower band gap energy [1, 3]. TiO_2-based photocatalysts are usually employed either as slurry or on support. In slurry condition, a big challenge lies in the separation and recovery of the small-sized particles after treatment of pollutants, which limits the application of the photocatalyst in real conditions. The utilization of support immobilization such as glass fibers, glass beads, or steel has also been employed. However, they have issue due to adhesion force between the photocatalyst surface and the support [9]. Recently, there are increasing interests in

a synergetic approach. Different materials are usually designed to provide a high surface area to support the catalyst [8, 10]. These materials share some common characteristics: binding to the catalyst, nondestroying catalyst, high surface area, and high affinity to the adsorption of pollutant molecules [10]. Activated carbon is one of the cost-effective synergist with not only clutching the photo-agents and free radicals ($HO^{\cdot}$) but also adsorbing pollutant molecules on the photochemical centers of the catalyst apart from its mechanical stability [10]. There are surprisingly quite a few papers using this method, and there is no published work on C/Fe co-doped titanium dioxide coated on activated carbon that is reported in this manuscript. Hence, in the present work, TiO_2 co-doped iron and carbon coated on activated carbon that was treated by HNO_3 was prepared by sol-gel followed by solvothermal method. The characterization of the catalyst was conducted by X-ray photoelectron spectroscopy (XPS), X-ray diffraction (XRD), infrared spectroscopy (IR), transmission electron microscopy (TEM), high-resolution transmission electron microscopy (HR-TEM), ultraviolet-visible (UV-Vis) spectroscopy, and Brunauer–Emmett–Teller (BET) surface area measurement. The catalytic activity of the catalyst was examined by the degradation of RhB dye.

2. Experimental

2.1. Catalyst Preparation

2.1.1. Chemicals. TIOT (tetraisopropyl orthotitanate 98%), nitric acid (HNO_3 68%), ethyl alcohol (C_2H_5OH 99.7%), iron (III) nitrate ($Fe(NO_3)_3.9H_2O$ pure), and rhodamine B ($C_{28}H_{31}ClN_2O_3$) were purchased from Sigma-Aldrich. Activated carbon Tra Bac (AC—particle sizes from 0.075 mm to 4.75 mm, surface area BET 928 m^2/g) was obtained with the aid of a TriStar 3000 V6.07 A.

2.1.2. Preparation of Fe-C-TiO_2 Coated on Activated Carbon Pretreated by HNO_3 (Fe-C-TiO_2/AC)

(i) Treatment of carbon with HNO_3: The coal is ground to a fine powder 0.16 mm before being washed with water and boiled for 2 hours to eliminate gases such as O_2, CO_2, and SO_2. Next, extracted carbon was immersed into HNO_3 12M and stirred for 3 hours at room temperature and then soaked for 24 hours. Finally, activated carbon (AC) was washed several times with distilled water and then dried for 3 hours at 100°C.

(ii) Preparation of Fe-C-TiO_2/AC: 6 mL of TIOT was added into 34 mL of ethylic alcohol to make solution A. Solution B was prepared from 17 mL of ethanol, 0.4 mL of nitric acid (68%), 1.6 mL distilled water, 48.2 mg of $Fe(NO_3)_3.9H_2O$, and 0.2 g of AC. The solution A was dropped into solution B under slow stir for 14 hours at room temperature and left for gelation for 2 days before being autoclaved in a Teflon vessel for 10 hours at 180°C. The resulted powder was washed and dried at 100°C for 24 hours to obtain the Fe-C-TiO_2/AC catalyst.

2.2. Characterization of As-Synthesized Photocatalyst. The crystal structure of catalyst was determined by XRD (D8-Advance 5005). Transmission electron microscope (TEM, JEOL JEM-1010 electron Microscope) and high-resolution transmission electron microscopy (HR-TEM, Hitachi H-9000 NAR, Japan Advanced Institute of Science and Technology) were used to investigate the particle size and morphology of the samples. XPS spectra of the prepared samples were measured by an X-ray photoelectron spectroscopy (XPS) (Kratos Axis Ultra—Frederick Seitz Materials Research laboratory-University of Illinois, Urbana-Champaign, USA). The absorbance was conducted by UV-Vis spectroscopy (Tasco-V670 photospectrometer). Functional groups were identified by IR spectroscopy (IR prestige 21). Nitrogen isothermal adsorption (Brunauer–Emmett–Teller (BET)) was determined by TriStar 3000 V6.07 A. Rhodamine B (RhB) concentrations were determined by a UV-Vis spectroscopy at the wavelength of 553 nm (the absorption maximum wavelength of RhB).

2.3. Photocatalytic Performance of As-Synthesized Photocatalysts. The catalytic activity of prepared materials was examined by the degradation of RhB solution (20 mg/L) under visible-light irradiation. The compact light (36W) was used instead of solar light with a range of wavelengths from 400 to 700 nm. An appropriate amount of catalyst (1–3 g/L) was added into 100 mL of RhB solution in a 250 mL beaker. The mixture was mixed at a constant rate in the dark for 30 minutes to ensure the desorption/adsorption equilibrium before being irradiated. After certain periods of time, the mixtures were sampled to determine the RhB concentrations by the UV-Vis spectroscopy.

3. Results and Discussion

3.1. Characterization of Synthesized Photocatalysts. Overall XPS spectra of principal elements Ti 2p, O 1s, C 1s, N 1s, and Fe 2p in synthesized photocatalysts are presented in Figure 1(a). The high-resolution scan over Ti 2p, O 1s, C 1s, N 1s, and Fe 2p spectral regions is shown in Figures 1(b)–1(f), respectively. The Ti 2p spectrum consists of peaks located at 459.1 eV and 464.8 eV, indicating the existence of Ti (IV) in TiO_2 component [1]. This suggests that the doping of iron and carbon then attached to the AC carrier does not alter the chemical state of TiO_2. This result is consistent with the XRD results (Figure 2). O 1s spectrum consists of the main peak at 529.9 eV and shoulder peak at 531.9 eV. These peaks correspond to Ti-O bond and O-H groups in TiO_2 [8]. This hydrogen hydroxyl group is useful for adsorption of organic substances or it can capture photogenic holes to form $HO^{\bullet}$ free radicals that increase photocatalytic activity of photocatalysts.

The presence of peaks at 711.1 eV and 723.1 eV is attributed to Fe^{III} $2p_{3/2}$ and Fe^{III} $2p_{1/2}$; it is possible to predict the presence of iron in Fe^{3+} oxidation state. In addition, there is also the binding energy value at 709.2 eV corresponding to Fe^{II} $2p_{3/2}$, which characterizes the existence of Fe^{2+} ions, possibly in FeO [5]. Coexistence of Fe^{3+} and Fe^{2+}

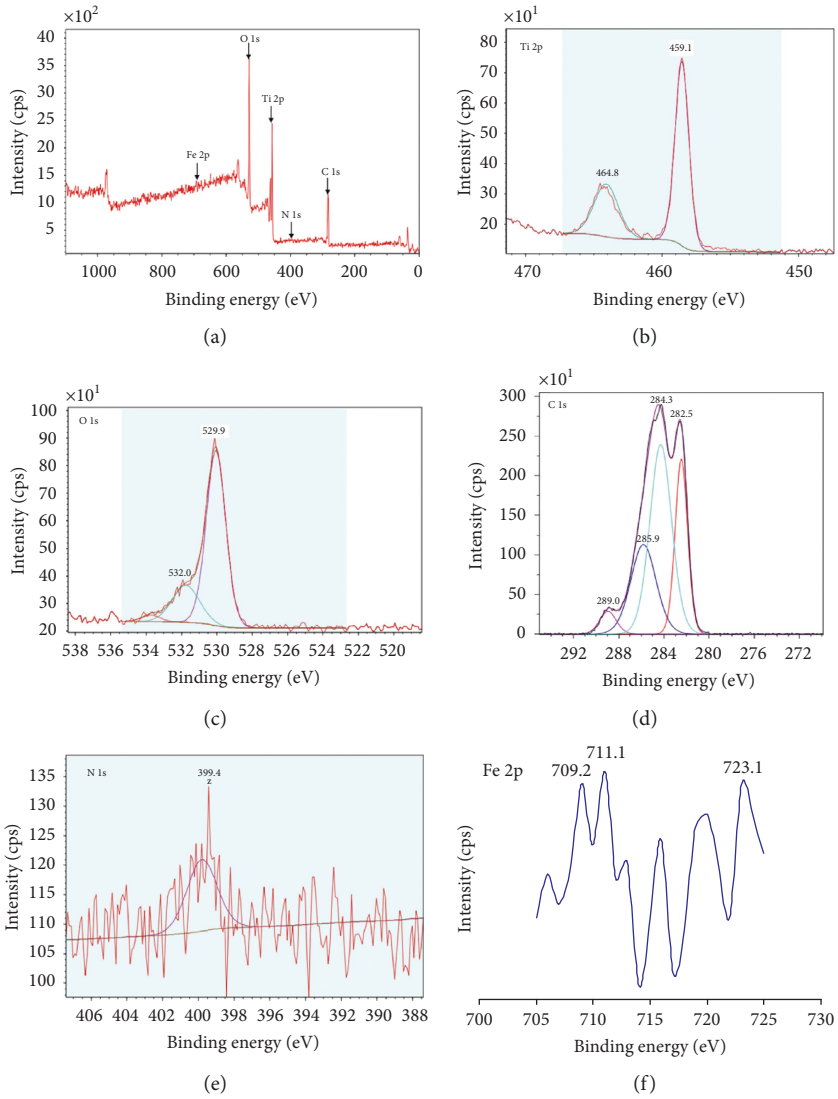

Figure 1: XPS spectra of Fe-C-TiO_2/AC (a), Ti 2p (b), O 1s (c), C 1s (d), N 1s (e), and Fe 2p (f).

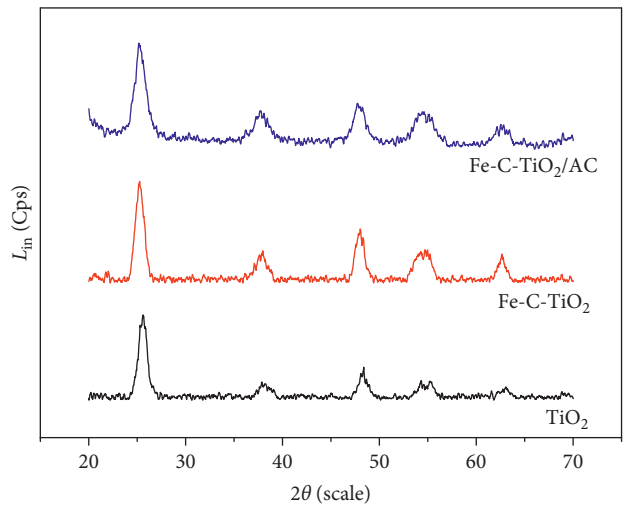

Figure 2: XRD patterns of Fe-C-TiO_2/AC, Fe-C-TiO_2, and TiO_2.

can enhance the photocatalytic efficiency based on the following reactions:

$$\begin{aligned} Fe^{2+} + O_{ads} &\longrightarrow Fe^{3+} + O^{-}{}_{ads} \\ Fe^{3+} + e^{-}CB &\longrightarrow Fe^{2+} \end{aligned} \quad (1)$$

in which Fe^{3+} acts as a conductive photonic electron trap to prevent recombination of electrons and holes, while Fe^{2+} provides electrons to adsorb oxygen on the catalytic surface and helps the charge transfer on the surface faster [1, 5].

Typical peaks of C are shown in Figure 1(d). The main peak with energy value at 284.3 eV is assigned to carbon graphite. The presence of 285.9 eV and 288.4 eV peaks is associated with C-O and C=O bonds of catalytic surface carbonates [11]. The existence of this carbonate radical increases the sensitivity for catalysis, because of the involvement of carbon-containing functional groups in activated carbon [1]. A peak at 282.5 eV corresponds to the Ti-C bond in the nanocrystalline catalyst attached to AC, and this link proves that part of the carbon is involved in replacing the oxygen in the network TiO_2 anatase crystals. The XPS analysis confirmed that iron and carbon had successfully entered the TiO_2 network and also showed the successful binding of catalyst to activated carbon activated by HNO_3.

The XRD patterns (Figure 2) show that Fe-C-TiO_2 after being coated on activated carbon exhibits the typical peaks referring to the anatase form [6]. The phase composition of nanoscale particles is preserved compared with the original materials (Figure 3).

The TEM images of the Fe-C-TiO_2/AC sample (Figure 3(a)) show that the catalyst system contains very fine particles, with typical size of 5 nm, evenly distributed on the surface of activated carbon. The result of HR-TEM (Figure 3(b)) confirms the Fe-C-TiO_2 catalyst binding on AC is based on black spots covered by catalytic spheres [10].

Proposed mechanism of TiO_2 coating process on AC is shown in Figure 4. After AC was pretreated with HNO_3, carbon supplied more hydroxyl and acid groups on the surface, which bond to OH^- and H^+ ions of catalyst to enhance the adhesiveness.

Table 1 shows that the surface areas of pristine AC and AC carrying catalysts measured by BET are different. The reason is that during the treatment of AC, HNO_3 is a strong oxidant, leading to changes in porous structure, which might reduce the number of small capillaries and increase the number of large ones, therefore reducing the surface area.

IR spectra of pristine TiO_2, Fe-C-TiO_2, and Fe-C-TiO_2/AC are presented in Figure 5. Peak at 1436 cm^{-1} refers to the -COO-Ti vibration. The peaks at 551 cm^{-1} and 502–505 cm^{-1} are assigned to the bonds of Ti-O and Ti-O-C, respectively.

The UV-Vis spectra of the samples are displayed in Figure 6. The results show that by coating Fe-C-TiO_2 on AC, the absorption band of Fe-C-TiO_2/AC was significantly expanded to the visible region in comparison with the absorption band of pristine TiO_2 and Fe-C-TiO_2. Indeed, as expected, the main absorption edge of TiO_2 was estimated to be about 398 nm (2.96 eV) due to its intrinsic band gap absorption. The onset of the absorption spectrum of Fe-C-TiO_2 was shifted to the visible region because of the Fe and C dopants while Fe-C-TiO_2/AC presented main absorption spectrum at the region above 480 nm. This result suggests that the Fe-C-TiO_2/AC catalyst is more active under visible light.

From the UV-Vis spectra of pristine TiO_2, Fe-C-TiO_2, and Fe-C-TiO_2/AC (Figure 7), the band gap energies estimated from the intercept of the tangents to the plots by using Kubelka–Munk method were 2.96, 2.17, and 1.63 eV for pristine TiO_2, Fe-C-TiO_2, and Fe-C-TiO_2/AC, respectively.

3.2. Catalytic Activity of Fe-C-TiO_2/AC in the Degradation of RhB under Visible Light. The comparison of photocatalytic performance of Fe-C-TiO_2/AC, Fe-C-TiO_2, and TiO_2 with that of pure AC in the degradation of RhB under visible-light irradiation with the same catalyst load (1.6 g/L) is presented in Figure 8. AC adsorbs RhB and reaches the equilibrium after 60 min of reaction, which can be proved by unchanged RhB concentration over time. The results also indicate that Fe-C-TiO_2/AC is the best photocatalyst in degradation of RhB in solutions with more than 99% of RhB removal after 90 min while pristine TiO_2 exhibits the lowest performance (only some 40% of RhB is removed after the same reaction time). Pure AC and Fe-C-TiO_2 present photocatalytic efficiency in between pristine TiO_2 and Fe-C-TiO_2/AC. This illustrates the synergy between adsorption capacity of AC and the improvement of Fe-C-TiO_2 compared with pristine TiO_2.

Figure 9 shows that the optimal catalyst load was 1.6 mg/L in the degradation of RhB in solutions while more dilute or concentrated catalyst concentrations will result in lower levels of RhB degradation. In fact, more than 99% of RhB was decomposed after 90 min of visible-light irradiation with a catalyst load of 1.6 mg/L while these figures for the catalyst loads at 1, 1.2, 1.4, 1.8, and 2.5 were, respectively, 40%, 50%, 53%, 78%, and 62%. This can be explained by the fact that the higher quantity of catalyst load may cause the light absorption hindrance, decreasing the efficiency of RhB degradation, whereas the lower catalyst load would lead to lower active sites ready for the degradation of the pollutant.

The photocatalytic degradation of RhB by the Fe-C-TiO_2/AC system can be explained by the following mechanism proposal (Figure 10): (1) when $h\nu \geq (E_C - E_V)$, then electrons would be excited in the valence band of TiO_2 by the process: $TiO_2 + h\nu\ (UV) \longrightarrow TiO_2\ (e_{CB}- + h_{VB}+)$; (2) when $(E_C - E'_V) \leq h\nu < (E_C - E_V)$, electrons can be excited from the Fe-C-TiO_2/AC energy level by the following process: Fe-C-TiO_2/C + hν (visible) ⟶ Fe-C-TiO_2/AC ($e_{CB}- + h_{VB}+$); and (3) when $(E'_V - E_V) \leq h < (E_C - E_W)$, electrons would be excited and moved from the valence band of TiO_2 to the Fe-C-TiO_2/AC energy level by the process: TiO_2 + Fe-C-TiO_2/C + hν (visible) ⟶ Fe-C-TiO_2/AC ($e_{CB}-$) + TiO_2 ($h_{VB}+$). The departed electrons and holes subsequently migrate to the surface of the catalysts and react with adsorbed H_2O and O_2 molecules, forming $HO^{\cdot}$ and $O_2^{\cdot}$, respectively. $HO^{\cdot}$ and $O_2^{\cdot}$ radicals are mainly responsible for the degradation of RhB in solution [12].

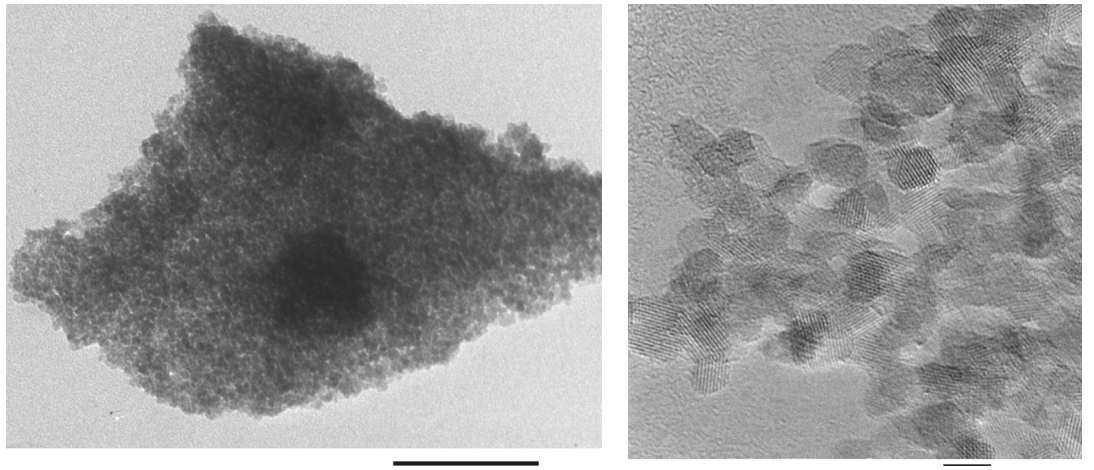

(a) (b)

Figure 3: TEM images of Fe-C-TiO_2/AC (a) and HR-TEM of Fe-C-TiO_2/AC (b).

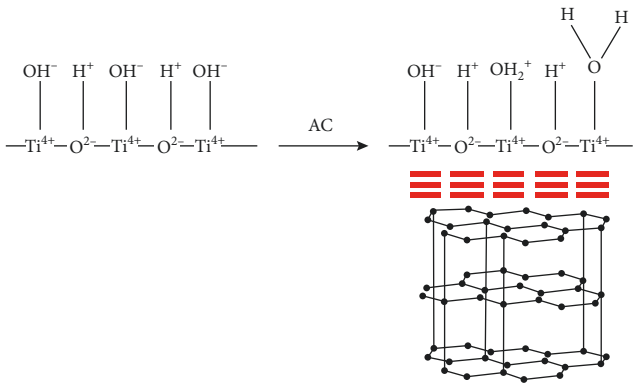

Figure 4: Proposed mechanism of TiO_2 coating process on AC.

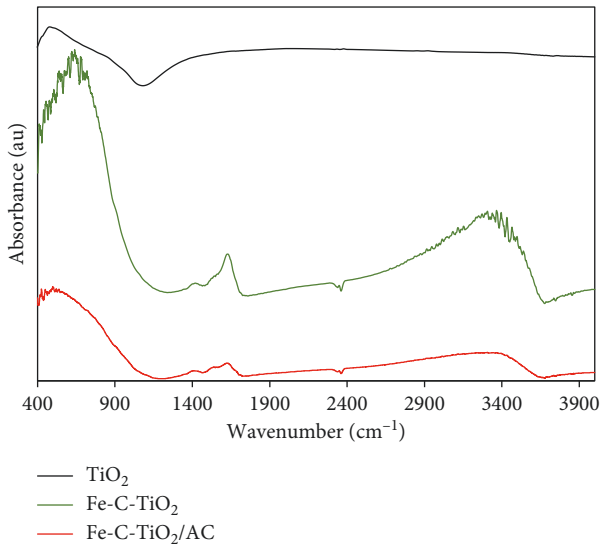

Figure 5: IR spectra of Fe-C-TiO_2/AC, Fe-C-TiO_2, and TiO_2.

Table 1: Physical properties of AC, Fe-C-TiO_2, and Fe-C-TiO_2/AC.

Materials	Mean size (nm) from the XRD results	BET surface area ($m^2 \cdot g^{-1}$)	V_p ($cm^3 \cdot g^{-1}$)
Fe-C-TiO_2/AC	5.13	264.8	0.30
Fe-C-TiO_2	4.23	237.2	0.23
AC	—	928.2	—

The catalytic stability in RhB decomposition under visible-light irradiation was studied. After each decomposition cycle (90 min), the catalyst was centrifuged and washed with distilled water and then used for further treatment of RhB in solution. The results show that the catalyst exhibited good photocatalytic activity after 5 cycles, as shown in Figure 11. The ability to decompose RhB over 5 cycles remained high (>87%). This research has proved that Fe-C-TiO_2/AC is a highly durable, economically suitable, and practical catalyst.

4. Conclusions

The Fe-C-TiO_2 catalyst was successfully carried on the AC treated by HNO_3. The nature of the catalyst remained to be unchanged regarding phase composition, particle sizes, and structure. Furthermore, the large surface area of AC adsorbs more organic molecules, leading to enhance the RhB degradation in solutions. The catalyst after being deposited on AC carriers activated with HNO_3 has better photocatalytic activity than activated carbon without catalysts. The Fe-C-TiO_2/AC catalyst also presented better photocatalytic performance in RhB degradation compared with pristine TiO_2 and with Fe-C-TiO_2. The optimal catalyst load for RhB

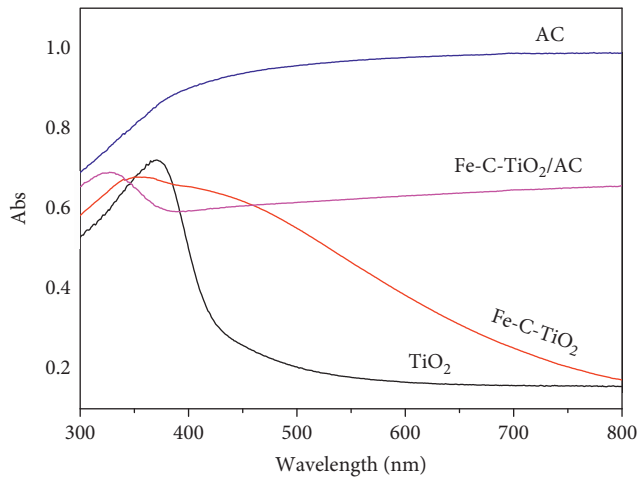

Figure 6: UV-Vis spectra of pure AC, Fe-C-TiO_2/AC, Fe-C-TiO_2, and TiO_2.

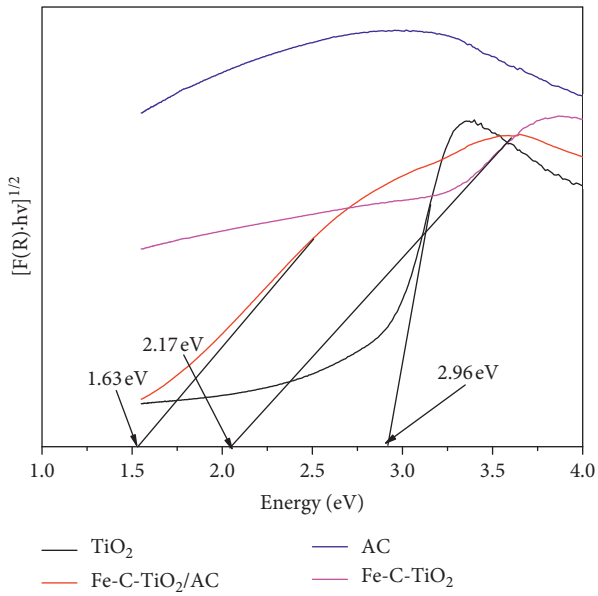

Figure 7: Plot of $[F(R)\cdot h\nu]^{1/2}$ vs energy (eV) for pure AC, Fe-C-TiO_2/AC, Fe-C-TiO_2, and TiO_2.

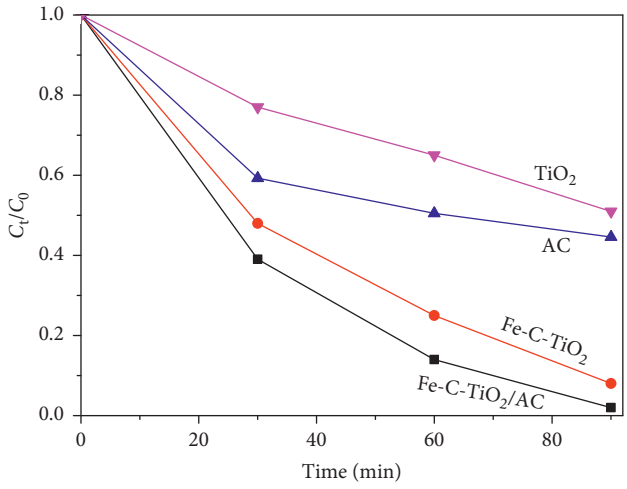

Figure 8: Comparison of photocatalytic activity of Fe-C-TiO_2/AC, Fe-C-TiO_2, and TiO_2 with that of pure AC.

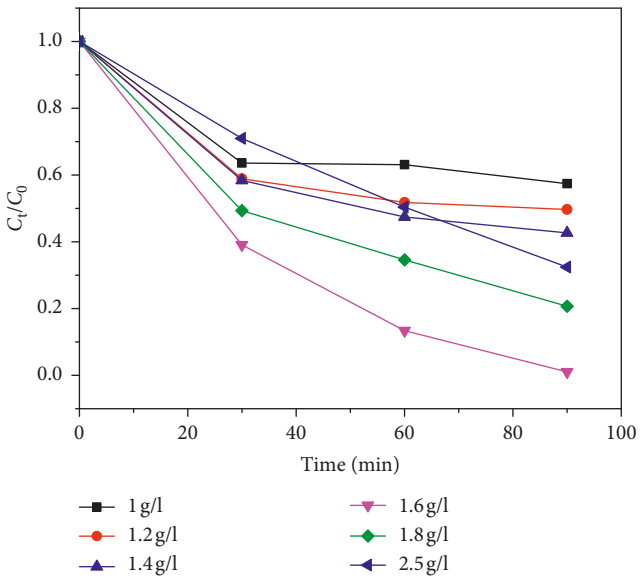

Figure 9: Optimization of catalyst load in the degradation of RhB by Fe-C-TiO_2/AC.

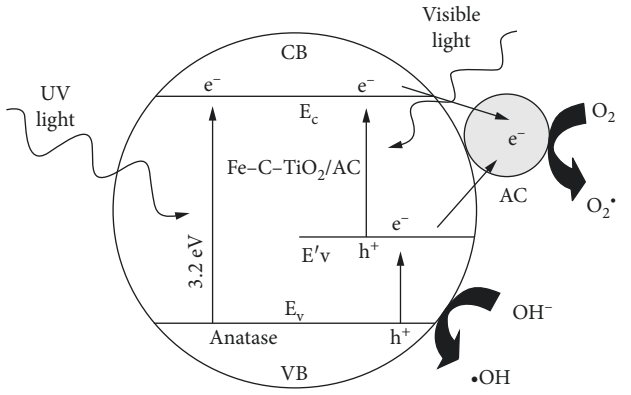

Figure 10: Schematic mechanism of photocatalytic degradation of RhB by Fe-C-TiO_2/AC (adopted from [12]).

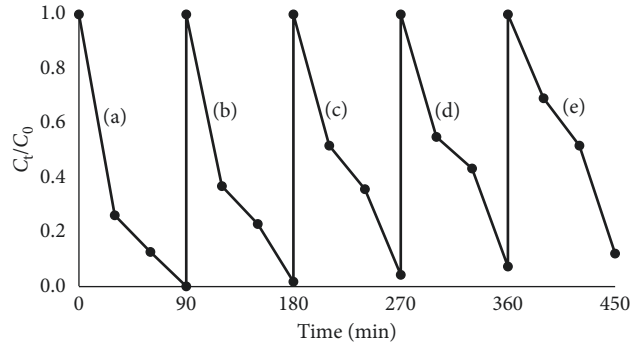

Figure 11: Photocatalytic recycling of Fe-C-TiO_2/AC in RhB decomposition: first cycle (a); second cycle (b); third cycle (c); fourth cycle (d); fifth cycle (e).

decomposition (initial concentration of 20 mg/L) was found to be of 1.6 g/L. The catalysts with larger size favor the catalyst separation from solution and recycling. The Fe-C-TiO_2 carried on AC sample is a potential catalyst in degradation of toxic organic compounds under visible-light irradiation.

Data Availability

The data used to support the findings of this study are included within the article.

Conflicts of Interest

The authors declare that there are no conflicts of interest regarding the publication of this paper.

Acknowledgments

This work was partly supported by the team project of VLIR-UOS with code number ZEIN2016PR431. The authors would like to thank the RoHan project for the utilization of instruments.

References

[1] X. Wang, Y. Tang, M.-Y. Leiw, and T.-T. Lim, "Solvothermal synthesis of Fe-C codoped TiO_2 nanoparticles for visible-light photocatalytic removal of emerging organic contaminants in water," *Applied Catalysis A: General*, vol. 409-410, pp. 257–266, 2011.

[2] S. Jafari, B. Tryba, E. Kusiak-Nejman, J. Kapica-Kozar, A. W. Morawski, and M. Sillanpää, "The role of adsorption in the photocatalytic decomposition of Orange II on carbon-modified TiO_2," *Journal of Molecular Liquids*, vol. 220, pp. 504–512, 2016.

[3] Y. Wu, J. Zhang, L. Xiao, and F. Chen, "Properties of carbon and iron modified TiO_2 photocatalyst synthesized at low temperature and photodegradation of acid orange 7 under visible light," *Applied Surface Science*, vol. 256, pp. 260–268, 2010.

[4] Z. Hu, T. Xu, and B. Fang, "Photocatalytic degradation of vehicle exhaust using Fe-doped TiO_2 loaded on activated carbon," *Applied Surface Science*, vol. 420, pp. 34–42, 2017.

[5] Y. Li, J. Chen, J. M. Liu, M. Ma, W. Chen, and L. Li, "Activated carbon supported TiO_2-photocatalysis doped with Fe ions for continuous treatment of dye wastewater in a dynamic reactor," *Journal of Environmental Sciences*, vol. 22, no. 8, pp. 1290–1296, 2010.

[6] A. Eshaghi and H. Moradi, "Optical and photocatalytic properties of the Fe-doped TiO_2 nanoparticles loaded on the activated carbon," *Advanced Powder Technology*, vol. 29, no. 8, pp. 1879–1885, 2018.

[7] N. C. Birben, C. S. Uyguner-Demirel, S. S. Kavurmaci et al., "Application of Fe-doped TiO_2 specimens for the solar photocatalytic degradation of humic acid," *Catalysis Today*, vol. 281, no. 1, pp. 78–84, 2017.

[8] P.-S. Yap and T.-T. Lim, "Effect of aqueous matrix species on synergistic removal of bisphenol-A under solar irradiation using nitrogen-doped TiO_2/AC composite," *Applied Catalysis B: Environmental*, vol. 101, no. 3-4, pp. 709–717, 2011.

[9] Z. F. Shi, S. M. Zhang, and S. Guo, "Characteristics and photocatalytic activity of TiO," *Applied Mechanics and Materials*, vol. 295–298, pp. 413–417, 2013.

[10] D. Huang, Y. Miyamoto, J. Ding et al., "A new method to prepare high-surface-area N–TiO_2/activated carbon," *Materials Letters*, vol. 65, pp. 326–328, 2011.

[11] X. Cheng, X. Yu, and Z. Xing, "Synthesis and characterization of C-N-S-tridoped TiO_2 nano-crystalline photocatalyst and its photocatalytic activity for degradation of rhodamine B," *Journal of Physics and Chemistry of Solids*, vol. 74, pp. 684–690, 2013.

[12] L. Youji, Z. Xiaoming, C. Wei et al., "Photodecolorization of Rhodamine B on tungsten-doped TiO_2/activated carbon under visible-light irradiation," *Journal of Hazardous Materials*, vol. 227, no. 228, pp. 25–33, 2012.